

Effects of the higher partial waves and relativistic terms on the accuracy of the calculation of the hypertriton electroproduction

T. Mart

Departemen Fisika, FMIPA, Universitas Indonesia, Depok 16424, Indonesia

Abstract

We have investigated the accuracies of calculations made by omitting the higher partial waves of nuclear wave functions and the elementary relativistic terms in the hypertriton electroproduction. We found that an accurate calculation would still be obtained if we used at least three lowest partial waves with isospin $T = 0$. Furthermore, we found that the omission of the relativistic terms in the elementary process amplitude could lead to a large deviation from the full calculation. We also present the cpu-times required to calculate the cross sections. For future consideration the use of these lowest partial waves is suggested, since the calculated cross section deviates only about 0.17 nb/sr ($\approx 4\%$), at most, from the full calculation, whereas the cpu-time is reduced by a factor of 60. Comparison of our result with the available experimental data supports these findings.

Key words: Meson electroproduction, partial waves, hypernuclei

PACS: 13.60.Le, 25.30.Rw, 21.80.+a

1. Introduction

An accurate calculation using a simple formalism is naturally desired in all phenomenological studies of nuclear and particle physics. However, in most cases this is difficult to achieve, because an accurate calculation usually does not allow for any extreme approximation. Therefore, an optimal approximation which only includes the most important parts of the formalism, without sacrificing the accuracy of the numerical result, should be obtained. A good example is found in the analysis of the hypertriton photo- and electroproduction, i.e.,

$$\gamma + {}^3\text{He} \rightarrow K^+ + {}^3_{\Lambda}\text{H} \quad \text{and} \quad e + {}^3\text{He} \rightarrow e' + K^+ + {}^3_{\Lambda}\text{H},$$

given in Refs. [1, 2]. In this analysis the cross section is calculated by means of the elementary operator Kaon-Maid [3] sandwiched between two nuclear wave functions (${}^3\text{He}$ and ${}^3_{\Lambda}\text{H}$) obtained from the solutions of Faddeev equations using modern nucleon-nucleon and hyperon-nucleon potentials [4, 5]. The numbers of partial waves for the ${}^3\text{He}$ and ${}^3_{\Lambda}\text{H}$ wave functions are 34 and 16, respectively.

Along with the corresponding probabilities these partial waves are shown in Table 1. In both wave functions the total numbers of supporting points for the two-body (\mathbf{p}) and the spectator (\mathbf{q}) momenta are 34 and 20, respectively. As we shall see in the next Section, this could lead to a problem of integration with almost two billions grid points. Therefore, it is obviously very important to limit the number of participating partial waves or to truncate the elementary amplitude in order to simplify the formalism as well as to avoid the unnecessarily long cpu-time required to calculate the reaction cross section. At $W = 4.04$ GeV it has been shown in Ref. [1] that for the hypertriton photoproduction the use of four lowest partial waves ($\alpha \leq 4$, see Table 1 for the explanation of α) would nicely approximate the full calculation, whereas the use of $\alpha \leq 5$ would lead to a perfect result. It has been also pointed out that careful inspections in a wide range of kinematics should be performed, before we can apply this approximation in the hypertriton photo- and electroproduction [1].

Furthermore, it has been also known that the hypernucleus production cross section is sensitive to the elementary amplitude, especially at the forward directions, where the two recent experimental data sets from SAPHIR [6] and CLAS [7] collaborations show a lack of mutual consistency [8]. As a consequence, hypertriton production at this kinematics could also shed light on the solution of this discrepancy problem. However, the extraction of the information on the elementary amplitude from the nuclear cross sections requires a massive fitting process, which would become impossible if the cpu-times required to calculate these cross sections were extremely long.

The present analysis is greatly motivated by these facts. Here we shall quantitatively investigate the effects of omitting the higher partial waves of nuclear wave functions on the accuracy of the calculation. We shall also compare this result with the result of the approximation made by excluding the relativistic terms in the elementary amplitude as suggested in Ref. [9]. To this end we take the electroproduction process, since photoproduction is only a special case of electroproduction. Our motivation is obvious, namely to find the shortest cpu-time for which the deviation of the calculated cross section from the full calculation is still controllable.

This paper is organized as follows: In Section 2 we shall briefly review our formalism and state our problem. We shall present and discuss the results of our calculations in Section 3. Section 4 will focus on the comparison of our results with experimental data. In Section 5 we shall summarize our findings.

2. Formalism and Statement of the Problem

The formalism of the hypertriton electroproduction off ${}^3\text{He}$ in an impulse approximation has been presented in Ref. [1]. Except for the difference between the initial and final nuclear masses, as well as between the initial proton and the final hyperon masses in the elementary operator, the formulas are similar to those used in pion electroproduction off ${}^3\text{He}$ [10]. To facilitate the discussion, here we will only present the most important part of them. We start with the

Table 1: Quantum numbers and probabilities (in %) of the ${}^3\text{He}$ and the hypertriton wave functions [4, 5].

α	L	S	J	l	$2j$	$2T$	$P({}^3\text{He})$	$P({}^3_{\Lambda}\text{H})$
1	0	0	0	0	1	1	44.580	-
2	0	1	1	0	1	0	44.899	93.491
3	2	1	1	0	1	0	2.848	5.794
4	0	1	1	2	3	0	0.960	0.034
5	2	1	1	2	3	0	0.189	0.027
6	1	0	1	1	1	0	0.089	0.004
7	1	0	1	1	3	0	0.198	0.008
8	1	1	0	1	1	1	1.107	-
9	1	1	1	1	1	1	1.113	-
10	1	1	1	1	3	1	0.439	-
11	1	1	2	1	3	1	0.064	-
12	3	1	2	1	3	1	0.306	-
13	1	1	2	3	5	1	1.018	-
14	3	1	2	3	5	1	0.024	-
15	2	0	2	2	3	1	0.274	-
16	2	0	2	2	5	1	0.425	-
17	2	1	2	2	3	0	0.122	0.024
18	2	1	2	2	5	0	0.095	0.018
19	2	1	3	2	5	0	0.205	0.053
20	4	1	3	2	5	0	0.053	0.006
21	2	1	3	4	7	0	0.126	0.010
22	4	1	3	4	7	0	0.038	0.007
23	3	0	3	3	5	0	0.005	0.001
24	3	0	3	3	7	0	0.008	0.001
25	3	1	3	3	5	1	0.051	-
26	3	1	3	3	7	1	0.045	-
27	3	1	4	3	7	1	0.008	-
28	5	1	4	3	7	1	0.074	-
29	3	1	4	5	9	1	0.178	-
30	5	1	4	5	9	1	0.006	-
31	4	0	4	4	7	1	0.053	-
32	4	0	4	4	9	1	0.059	-
33	4	1	4	4	7	0	0.011	0.004
34	4	1	4	4	9	0	0.009	0.003

corresponding nuclear transition matrix element, which can be written as [1]

$$\langle {}^3_{\Lambda}\text{H} | J^{\mu} | {}^3\text{He} \rangle = \sqrt{3} \int d^3\mathbf{p} d^3\mathbf{q} \Psi_{\Lambda\text{H}}^*(\mathbf{p}, \mathbf{q}') J^{\mu}(\mathbf{k}, \mathbf{k}_1, \mathbf{k}'_1) \Psi_{3\text{He}}(\mathbf{p}, \mathbf{q}) , \quad (1)$$

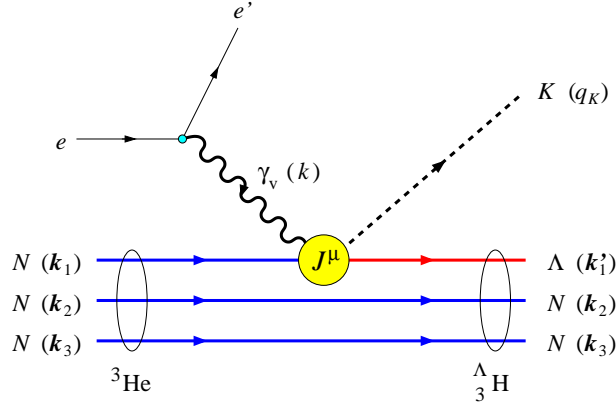


Figure 1: Electroproduction of the hypertriton on a ${}^3\text{He}$ target in an impulse approximation, where the virtual photon interacts with only one nucleon inside the ${}^3\text{He}$.

where the factor of $\sqrt{3}$ on the right hand side of Eq. (1) comes from the antisymmetry of the initial state, J^μ represents the elementary operator, while the integrations are taken over the three-body momentum coordinates (see Fig. 1 for the explanation of the momenta)

$$\mathbf{p} = \frac{1}{2}(\mathbf{k}_2 - \mathbf{k}_3) \quad , \quad \mathbf{q} = \mathbf{k}_1 \quad , \quad (2)$$

and the hyperon momentum in the hypertriton is given by

$$\mathbf{q}' = \mathbf{k}_1 + \frac{2}{3}(\mathbf{k} - \mathbf{q}_K) \quad . \quad (3)$$

By expanding the three-body wave functions in Eq. (1) in terms of their orbital momenta, spins, and isospins,

$$\begin{aligned} \Psi(\mathbf{p}, \mathbf{q}) &= \sum_{\alpha, \mathbf{m}} \phi_\alpha(p, q) (L m_L S m_S | J m_J) (l m_l \frac{1}{2} m_s | j m_j) (J m_J j m_j | \frac{1}{2} M_i) \\ &\times Y_{m_L}^L(\hat{\mathbf{p}}) Y_{m_l}^l(\hat{\mathbf{q}}) \chi_{m_S}^S \chi_{m_s}^{\frac{1}{2}} | (T \frac{1}{2}) \frac{1}{2} M_t \rangle \quad , \quad (4) \end{aligned}$$

we can recast the transition matrix element in Eq. (1) into the form

$$\begin{aligned} \langle {}^3_\Lambda\text{H} | J^\mu | {}^3\text{He} \rangle &= \sqrt{3} \sum_{\alpha, \alpha'} \sum_{\mathbf{m} \mathbf{m}'} (L m_L S m_S | J m_J) \\ &\times (L m_L S m_S | J' m_{J'}) (l m_l \frac{1}{2} m_s | j m_j) \\ &\times (l' m_{l'} \frac{1}{2} m_{s'} | j' m_{j'}) (J m_J j m_j | \frac{1}{2} M_i) \\ &\times (J' m_{J'} j' m_{j'} | \frac{1}{2} M_i) \delta_{LL'} \delta_{m_L m_{L'}} \delta_{SS'} \delta_{m_S m_{S'}} \delta_{T0} \\ &\times \int p^2 dp \, d^3 \mathbf{q} \phi_{\alpha'}(p, q') \phi_\alpha(p, q) Y_{m_{l'}}^{l'}(\hat{\mathbf{q}}') Y_{m_l}^l(\hat{\mathbf{q}}) \\ &\times \langle \frac{1}{2}, m_{s'} | J^\mu | \frac{1}{2}, m_s \rangle \quad , \quad (5) \end{aligned}$$

where α and α' indicate the partial waves of the initial and final nuclear wave functions, respectively, while the notations $\mathbf{m} = (m_L m_S m_l m_s m_J m_j)$ and $\mathbf{m}' = (m_{L'} m_{S'} m_{l'} m_{s'} m_{J'} m_{j'})$ have been introduced for the sake of brevity.

From Table 1 we can estimate that a full calculation of the four-dimensional integrals in Eq. (5) using all partial waves could involve integrations with $34 \times 16 \times 34 \times 20 \times 30 \times 10 = 110,976,000$ grid points, where the two last numbers in the multiplications (30×10) come from the minimum Gauss supporting points for the numerically-stable angular integrations [1].

It is also important to note that these integrations are performed over all components of the transition matrix element in the form of 4×4 matrix $[j^\mu]_{m_n}^{(n)}$ (or equivalently $[j_{\mu\nu}]$), where

$$\begin{aligned} J^\mu &= \sum_{n=0}^1 \sum_{m_n=-n}^{+n} (-1)^{m_n} \sigma_{-m_n}^{(n)} [j^\mu]_{m_n}^{(n)} \\ &= (1, \sigma_x, \sigma_y, \sigma_z) \begin{pmatrix} j_{00} & j_{x0} & j_{y0} & j_{z0} \\ j_{0x} & j_{xx} & j_{yx} & j_{zx} \\ j_{0y} & j_{xy} & j_{yy} & j_{zy} \\ j_{0z} & j_{xz} & j_{yz} & j_{zz} \end{pmatrix}. \end{aligned} \quad (6)$$

As a consequence, the problem of calculating the cross section becomes numerically more challenging, since it is equivalent to the problem of integration with 1,775,616,000 grid points. Furthermore, the result of this integration must be summed over angular-momentum and spin projections $m_J, m_{J'}, m_S$, and m_s [indicated by \mathbf{m} and \mathbf{m}' in Eq. (5)]. Fortunately, the selection rule represented by the three Kronecker delta functions in Eq. (5) along with current conservation reduce this number to about 156 millions grid points. Nevertheless, this still indicates a time-consuming numerical computation.

On the other hand, the elementary operator of the elementary process $\gamma_\nu(k) + p(p_p) \rightarrow K^+(q_K) + \Lambda(p_\Lambda)$ can be written as

$$\begin{aligned} \langle \Lambda | \epsilon_\mu J^\mu | p \rangle &= \sqrt{\frac{\epsilon_p \epsilon_\Lambda}{4m_p m_\Lambda}} \chi_\Lambda^\dagger \left[F_1 \boldsymbol{\sigma} \cdot \boldsymbol{\epsilon} + F_2 \boldsymbol{\sigma} \cdot \mathbf{k} \epsilon_0 + F_3 \boldsymbol{\sigma} \cdot \mathbf{k} \mathbf{k} \cdot \boldsymbol{\epsilon} \right. \\ &\quad + F_4 \boldsymbol{\sigma} \cdot \mathbf{k} \mathbf{p}_p \cdot \boldsymbol{\epsilon} + F_5 \boldsymbol{\sigma} \cdot \mathbf{k} \mathbf{p}_\Lambda \cdot \boldsymbol{\epsilon} + \frac{1}{\epsilon_p} \left\{ F_6 \boldsymbol{\sigma} \cdot \mathbf{p}_p \epsilon_0 + F_7 \boldsymbol{\sigma} \cdot \mathbf{p}_p \mathbf{k} \cdot \boldsymbol{\epsilon} \right. \\ &\quad \left. + F_8 \boldsymbol{\sigma} \cdot \mathbf{p}_p \mathbf{p}_p \cdot \boldsymbol{\epsilon} + F_9 \boldsymbol{\sigma} \cdot \mathbf{p}_p \mathbf{p}_\Lambda \cdot \boldsymbol{\epsilon} + F_{14} \boldsymbol{\sigma} \cdot \boldsymbol{\epsilon} \boldsymbol{\sigma} \cdot \mathbf{k} \boldsymbol{\sigma} \cdot \mathbf{p}_p \right\} \\ &\quad + \frac{1}{\epsilon_\Lambda} \left\{ F_{10} \boldsymbol{\sigma} \cdot \mathbf{p}_\Lambda \epsilon_0 + F_{11} \boldsymbol{\sigma} \cdot \mathbf{p}_\Lambda \mathbf{k} \cdot \boldsymbol{\epsilon} + F_{12} \boldsymbol{\sigma} \cdot \mathbf{p}_\Lambda \mathbf{p}_p \cdot \boldsymbol{\epsilon} \right. \\ &\quad \left. + F_{13} \boldsymbol{\sigma} \cdot \mathbf{p}_\Lambda \mathbf{p}_\Lambda \cdot \boldsymbol{\epsilon} + F_{15} \boldsymbol{\sigma} \cdot \mathbf{p}_\Lambda \boldsymbol{\sigma} \cdot \boldsymbol{\epsilon} \boldsymbol{\sigma} \cdot \mathbf{k} \right\} \\ &\quad + \frac{1}{\epsilon_p \epsilon_\Lambda} \left\{ F_{16} \boldsymbol{\sigma} \cdot \mathbf{p}_\Lambda \boldsymbol{\sigma} \cdot \boldsymbol{\epsilon} \boldsymbol{\sigma} \cdot \mathbf{p}_p + F_{17} \boldsymbol{\sigma} \cdot \mathbf{p}_\Lambda \boldsymbol{\sigma} \cdot \mathbf{k} \boldsymbol{\sigma} \cdot \mathbf{p}_p \epsilon_0 \right. \\ &\quad + F_{18} \boldsymbol{\sigma} \cdot \mathbf{p}_\Lambda \boldsymbol{\sigma} \cdot \mathbf{k} \boldsymbol{\sigma} \cdot \mathbf{p}_p \mathbf{k} \cdot \boldsymbol{\epsilon} + F_{19} \boldsymbol{\sigma} \cdot \mathbf{p}_\Lambda \boldsymbol{\sigma} \cdot \mathbf{k} \boldsymbol{\sigma} \cdot \mathbf{p}_p \mathbf{p}_p \cdot \boldsymbol{\epsilon} \\ &\quad \left. + F_{20} \boldsymbol{\sigma} \cdot \mathbf{p}_\Lambda \boldsymbol{\sigma} \cdot \mathbf{k} \boldsymbol{\sigma} \cdot \mathbf{p}_p \mathbf{p}_\Lambda \cdot \boldsymbol{\epsilon} \right\} \chi_p, \end{aligned} \quad (7)$$

where the individual amplitudes F_i are given in Refs. [1, 2], ϵ_μ is the virtual photon polarization vector, $\epsilon_p = E_p + m_p$, and $\epsilon_\Lambda = E_\Lambda + m_\Lambda$.

From Eq. (7) it is obvious that the amplitudes $F_{16} - F_{20}$ and $F_6 - F_{15}$ originate from the “small-small” (SS) and “small-big” (SB) terms of the Dirac spinors, respectively, whereas the rest correspond to the “big-big” (BB) terms. It can be easily shown that the ratio between the “small” and “big” terms is of the order v/c (see, e.g., Ref. [12]). In pion photoproduction near threshold it has been widely known that only the leading Kroll-Ruderman term F_1 significantly contributes to the process. However, in kaon photo- and electroproduction the high threshold energy of the process could certainly change this picture. In view of this, it is certainly tempting to neglect the relativistic SS-terms in our formalism as well as to investigate the effects of the SB- and other terms on the calculated cross sections of the hypertriton electroproduction.

For the purpose of numerical computation we note that the cross section of the hypertriton electroproduction in the c.m. system can be written as

$$\frac{d\sigma_v}{d\Omega_K} = \frac{d\sigma_T}{d\Omega_K} + \epsilon_L \frac{d\sigma_L}{d\Omega_K} + \epsilon \frac{d\sigma_{TT}}{d\Omega_K} \cos 2\phi_K + \sqrt{2\epsilon_L(1+\epsilon)} \frac{d\sigma_{LT}}{d\Omega_K} \cos \phi_K, \quad (8)$$

with ϵ represents the virtual photon polarization, $\epsilon_L = -(k^2/\mathbf{k}^2)\epsilon$ and the individual cross sections can be written as

$$\frac{d\sigma_i}{d\Omega_K} = \alpha_e \frac{q_K}{K_L} \frac{M_{\Lambda\text{H}}^3}{2W} W_i, \quad (i = \text{T, L, TT, and LT}), \quad (9)$$

with $\alpha_e = e^2/4\pi$ and $K_L = (W^2 - M_{\text{He}}^2)/2M_{\text{He}}$. The nuclear structure functions W_i are given by

$$W_{\text{T}} = \frac{1}{4\pi} (W^{xx} + W^{yy}), \quad (10)$$

$$W_{\text{L}} = \frac{1}{4\pi} W^{00}, \quad (11)$$

$$W_{\text{TT}} = \frac{1}{4\pi} (W^{xx} - W^{yy}), \quad (12)$$

$$W_{\text{LT}} = \frac{1}{4\pi} (W^{0x} + W^{x0}), \quad (13)$$

where the spin averaged Lorentz tensor $W^{\mu\nu}$ is related to the nuclear transition matrix element given in Eq. (1) by

$$W^{\mu\nu} = \frac{1}{2} \sum_{s_i s_f} \langle {}^3_\Lambda\text{H} | J^\mu | {}^3\text{He} \rangle \langle {}^3_\Lambda\text{H} | J^\nu | {}^3\text{He} \rangle^*. \quad (14)$$

The kinematic chosen in this analysis is close to that of experimental data [11], because we want to explore the kinematics region that is experimentally accessible. The angular distribution will be limited in the range of $0^\circ \leq \theta_K \leq 31^\circ$, in which the magnitude of the cross section is sizeable. The total c.m. energy is limited to $3.5 \text{ GeV} \leq W \leq 5 \text{ GeV}$, since below this limit the cross section would be too small, whereas above this limit the elementary operator would lose its predictive power.

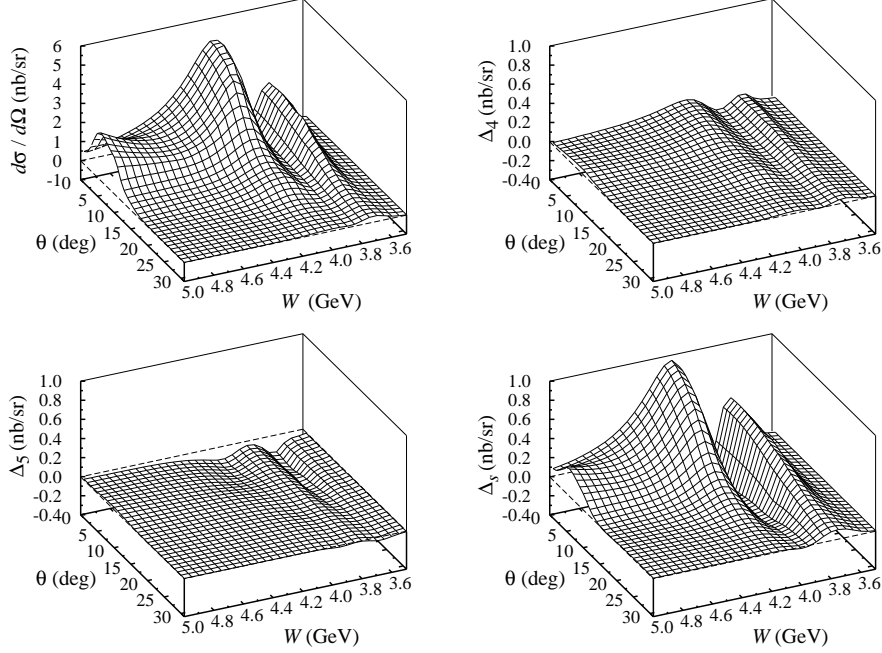


Figure 2: Effects of the higher partial waves on the differential cross section of the hypertriton electroproduction off ${}^3\text{He}$ at $k^2 = -0.35 \text{ GeV}^2$ and $\epsilon = 0.762$. The upper-left panel shows the result obtained from the full calculation by using all partial waves. Other panels display the differences between the full calculation and the calculation by using $\alpha \leq 5$ (Δ_5), $\alpha \leq 4$ (Δ_4), and only s -waves (Δ_s). Note that for the sake of visibility a different scale has been used for the vertical axis of the upper-left panel.

3. Results and Discussion

Figure 2 demonstrates the cross section obtained from the full calculation using all partial waves and the deviations from this result if we use $\alpha \leq 5$, $\alpha \leq 4$, and s -waves ($\alpha = 2, 4$). Our experience shows that computing the numerical data required by the plot of the differential cross section shown in the upper-left panel of Fig. 2 (consisting of $31 \times 31 = 961$ points) on a PC with a single processor Pentium-4 takes about 11 days (15,344 min).

From the lower-left panel of Fig. 2 it is obvious that limiting the partial waves up to $\alpha = 5$ yields an accurate approximation, since in general it just slightly underestimates the full calculation. The largest discrepancies are found at the two cross section peaks at $W \approx 3.75 \text{ GeV}$ and 4.10 GeV close to the forward angle, i.e., about 0.15 nb/sr (less than 3%). The average deviation over these 961 points is only 0.019 nb/sr . A similar behavior is also found if we use $\alpha \leq 4$, except in this case the calculated cross section slightly overestimates the cross section of the full calculation. Here, the average and largest deviations are found to be 0.038 nb/sr and 0.17 nb/sr (less than 4%), respectively. Finally,

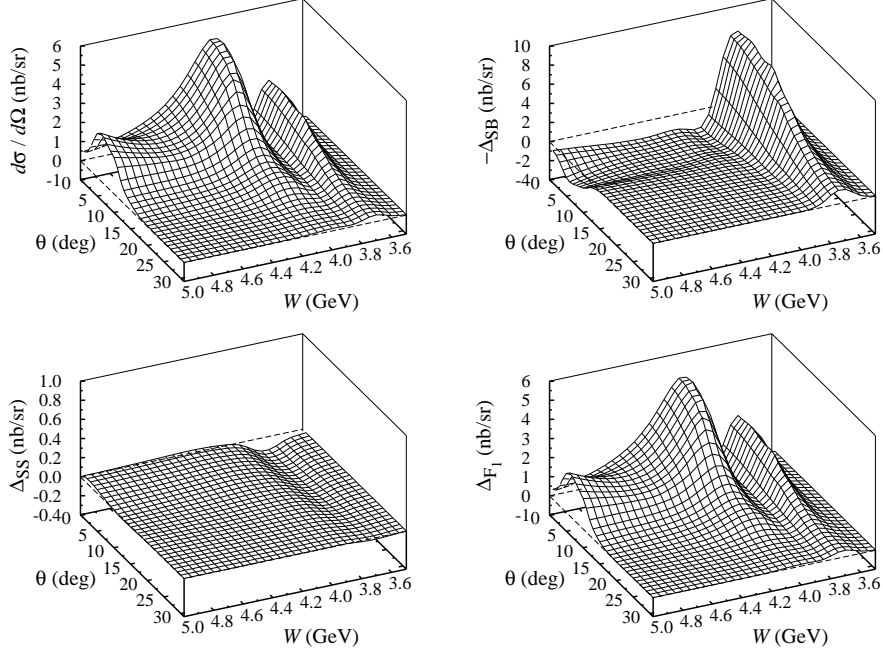


Figure 3: Effects of the relativistic terms on the differential cross section of the hypertriton electroproduction off ${}^3\text{He}$. The upper-left panel shows the result of a full calculation obtained by using all terms in Eq. (7), i.e., F_1 - F_{20} . Other panels display the differences between the full calculation and the calculation by using F_1 - F_{15} (Δ_{SS}), F_1 - F_5 (Δ_{SB}), and only F_1 (Δ_{F_1}). Note that all figures are obtained by using $\alpha \leq 5$ and the same kinematics as in Fig. 2. For the sake of visibility different scales have been used in vertical axes.

the largest deviation, almost 1 nb/sr at the top of the highest cross section peak, is obtained if we use only s -waves. Since the largest differential cross section is around 5 nb/sr, it is obvious that the latter provides a relatively poor approximation method for the hypertriton electroproduction.

Figure 3 demonstrates the effects of excluding the relativistic terms on the calculated differential cross section. Since it has just been shown that the use of $\alpha \leq 5$ can approximate the full calculation with an accuracy up to 3%, we believe that it is sufficient to limit the use of partial waves up to $\alpha \leq 5$ at this stage.

The lower-left panel of Fig. 3 demonstrates the effect of the SS-terms exclusion. We note that the maximum deviation is only about 4% at $W \approx 3.75$ GeV. Therefore, the SS-terms can be safely neglected for this process.

The shape of the differential cross section obtained by excluding the SB-terms is found to be completely different. As a consequence, the deviation from the full calculation is quite large (see also Table 2). The extreme nonrelativistic

Table 2: The cpu-time (τ) required to compute the numerical data of the cross section plot shown at the top panel of Fig. 2 along with the average and maximum deviations from the full calculation (indicated by $\Delta_{\text{av.}}$ and $\Delta_{\text{max.}}$, respectively) for different approximations, i.e., using all partial waves (Full), $\alpha \leq 5$ (1), $\alpha \leq 4$ (2), and only s -waves (3). With $\alpha \leq 5$ the role of different elementary amplitudes F_i given in Eq. (7) is demonstrated, i.e., using only $F_1 - F_{15}$ (a), $F_1 - F_5$ (b), and F_1 (c).

	Full	1	2	3	a	b	c
τ (min)	15,344	511	294	46	498	487	485
$\Delta_{\text{av.}}$ (nb/sr)	-	0.02	0.04	0.14	0.02	0.98	0.81
$\Delta_{\text{max.}}$ (nb/sr)	-	0.15	0.17	0.99	0.10	8.03	4.97

approximation (F_1 only) also yields a large deviation from the full calculation. The reason that the deviation in the latter is relatively smaller than in the former is that this approximation yields very small cross section. Although the analysis of Ref. [9] has been performed at the elementary level and using a quite different elementary operator, our result corroborates its finding, i.e., both the exclusion of the SB-terms and the extreme nonrelativistic approach can not be used as a good approximation in the hypertriton electroproduction. Furthermore since the exclusion of the SB-terms was not investigated by the authors of Ref. [9], our analysis therefore provides an extension of their finding.

At this stage, it is also important to consider the cpu-times required to make the plots just shown. Along with the corresponding deviations from the full calculation, the required cpu-times to calculate the 961 points of the cross section by using a single processor Pentium-4 PC are listed in Table 2.

It is interesting to see that the cpu-time is significantly reduced by a factor of 30 if we limit the partial waves up to $\alpha = 5$, while the accuracy is still maintained up to about 0.15 nb/sr. As a consequence, to obtain the plot shown at the top panel of Fig. 3 we need less than 9 hours. If we used the partial waves with $\alpha \leq 4$, the cpu-time is reduced by a factor of about 60, whereas the maximum deviation slightly increases to 0.17 nb/sr. The use of only s -waves substantially reduces the cpu-time, i.e., by a factor of 300. The average deviations displayed in Table 2 show in general the same behavior.

In contrast to the omission of the higher partial waves, the exclusion of the relativistic terms in Eq. (7) does not significantly reduce the cpu-times. This is clearly demonstrated in the first line of Table 2, where the cpu-time for the calculation with $\alpha \leq 5$ decreases from 511 min (full terms) to 485 min (only F_1). This result proves that computing the rest 19 F_i amplitudes in Eq. (7) is much simpler, and therefore much faster, than computing the massive integrals given in Eq. (5) with the complete partial waves. At the same time the maximum deviation in the latter becomes almost 5 nb/sr. This is because in the electromagnetic production of kaon the high energy of the process enhances the role of all but the Kroll-Ruderman term [see Eq. (7)], and the extreme

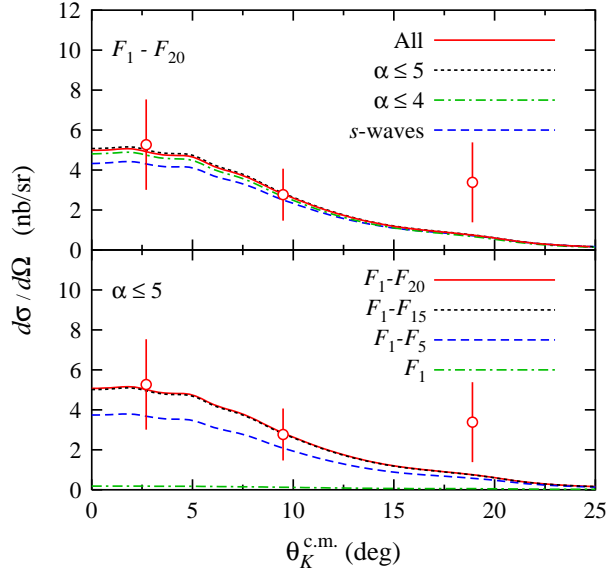


Figure 4: (Color online) Comparison between experimental data [11] and the calculation using all and specific numbers of partial waves (upper panel) and the approximations made by including only certain elementary amplitudes in the elementary operator (lower panel).

nonrelativistic approach results in a very small cross section. Consequently, the largest difference with the full calculation is about 5 nb/sr, i.e., the largest differential cross section found with the full calculation. Note that the decrease of Δ_{\max} from 0.15 nb/sr (full terms) to 0.10 nb/sr (using only $F_1 - F_{15}$) seems to be fortuitous, because the average deviations for the two cases are the same (0.02 nb/sr).

To complete our analysis we have also investigated the effects of the higher partial waves and the relativistic terms at $k^2 = -1.0 \text{ GeV}^2$. However, since the obtained cross sections are quite small (0.32 nb/sr, at most), it is very hard to draw a quantitative conclusion at this kinematics.

4. Comparison with experimental data

Although our primary motivation is to quantitatively study the effects of excluding higher partial waves and relativistic terms, it is also imperative to compare the results with the available experimental data given in Ref. [11]. The comparison is displayed in Fig. 4. Unfortunately, due to their large error bars, the present experimental data still allow for the s -wave approximation and the use of only BB terms in the elementary amplitude. In the latter, it is obvious that experimental data at forward angles with about 10% error bars would be able to justify the important role of the SB terms $F_6 - F_{15}$. In the former, we note that the largest deviation of using only s -waves does not appear at $W = 4.10$

GeV. Instead, at the forward directions the largest deviation (approximately $0.99 \mu\text{b}/\text{sr}$, see Fig. 2) is found with $W = 4.20$ GeV. Therefore, experimental data with the same quality, but at $W = 4.20$ GeV, would be very useful to check the validity of the s -waves approximation. For the sake of numerical accuracy and efficient cpu-time we would, however, recommend the use of partial waves with $\alpha \leq 4$ along with a full elementary amplitude.

The discrepancy between the calculated cross sections and the experimental data point at $\theta = 18.9^\circ$ requires a special explanation. At this kinematics we note that the calculated cross sections are much smaller than those at the forward direction. This behavior seems to be almost independent of the total c.m. energy. However, we have also found that the longitudinal part of the cross section ($d\sigma_L/d\Omega$) dominates other parts [see Eq. (8)] in the whole kinematics shown in Fig. 2 and falls off quickly as a function of the θ . On the other hand, the angular distribution of the transverse cross section ($d\sigma_T/d\Omega$) tends to be more flat than the longitudinal one. As a consequence, we may conclude that such behavior should originate from the elementary amplitude and not from the effect of the nuclear wave functions. Thus, if we believed that this experimental data point were correct, then we had to reconsider the improvement of the elementary operator. As stated in the Introduction, this means that the extraction of the elementary information from the hypertriton production cross section would be mandatory in the future works. Otherwise, new measurements at this kinematics are urgently required.

5. Conclusion

In conclusion, we have investigated the effects of higher partial waves and relativistic terms on the accuracy of the calculated differential cross sections of the hypertriton electroproduction. We have shown that an accurate calculation, with a maximum deviation of less than 4%, could still be obtained if we used the three lowest partial waves with isospin zero (i.e., using $\alpha \leq 4$, since the selection rule excludes the $\alpha = 1$ component). In this case, the cpu-time for calculating differential cross sections is reduced by a factor of about 60. The exclusion of certain elementary amplitudes F_i has a tiny impact on the cpu-time, but a big impact on the accuracy of the calculation. In view of this, for future consideration we suggest the use of partial waves with $\alpha \leq 4$ with a full elementary amplitudes F_i . Comparison of the results with the available experimental data supports our finding. New measurement of the hypertriton electroproduction with about 10% error bars would be very useful to clarify the validity of these approximations as well as the importance of the relativistic terms.

6. Acknowledgements

This work has been partially supported by the University of Indonesia.

References

- [1] T. Mart and B. I. S. van der Ventel, Phys. Rev. C 78 (2008) 014004.
- [2] T. Mart, L. Tiator, D. Drechsel, and C. Bennhold, Nucl. Phys. A640 (1998) 235.
- [3] T. Mart and C. Bennhold, Phys. Rev. C 61 (1999) 012201(R); T. Mart, Phys. Rev. C 62 (2000) 038201; C. Bennhold, H. Haberzettl and T. Mart, arXiv:nucl-th/9909022; T. Mart, C. Bennhold, H. Haberzettl, and L. Tiator, <http://www.kph.uni-mainz.de/MAID/kaon/kaonmaid.html>.
- [4] V. G. J. Stoks, R. A. M. Klomp, C. P. F. Terheggen, and J. J. de Swart, Phys. Rev. C 49 (1994) 2950.
- [5] K. Miyagawa and W. Glöckle, Phys. Rev. C 48 (1993) 2576.
- [6] K.-H. Glander *et al.*, Eur. Phys. J. A 19 (2004) 251.
- [7] R. Bradford *et al.*, Phys. Rev. C 73 (2006) 035202.
- [8] P. Bydžovský and T. Mart, Phys. Rev. C 76 (2007) 065202.
- [9] R. A. Adelseck, C. Bennhold and L. E. Wright, Phys. Rev. C 32 (1985) 1681.
- [10] L. Tiator and D. Drechsel, Nucl. Phys. A 360, 208 (1981).
- [11] F. Dohrmann *et al.*, Phys. Rev. Lett. 93 (2004) 242501.
- [12] F. Halzen and A. D. Martin, Quarks & Leptons: An Introductory Course in Modern Particle Physics (John Wiley & Sons, New York, 1984) p. 106.